COBALT BASED ALLOY OXIDATION AT HIGH TEMPERATURES

Henri Buscail, R. Rolland, F. Riffard, C. Issartel, S. Perrier

COBALT BASED ALLOY OXIDATION AT HIGH TEMPERATURES

H. BUSCAIL, R. ROLLAND, F. RIFFARD, C. ISSARTEL, S. PERRIER

LVEEM, Laboratoire Vellave sur l'Elaboration et l'Etude des Matériaux,
Clermont Université, UdA, rue Lashermes, BP 70219, 43006 Le Puy-en-Velay, France
henri.buscail@uca.fr, fax: +33 471 09 90 49

Abstract

The parabolic behaviour is followed during Phynox cobalt based alloy isothermal oxidation. The scale growth mechanism in air is limited by the diffusion process in a growing Cr_2O_3 oxide scale. Oxidation under thermal cycling conditions show that the best scale adherence is obtained at 1000°C. The good adherence is due to a rapid chromium supply from the substrate insuring a continuous chromia scale formation. At 1000°C, silicon and molybdenum promote the oxide scale keying at the internal interface. At 900 °C, the bad scale adherence is related to the cobalt oxidation and $CoCr_2O_4$ oxide formation. Thermal cycling tests at 1100 °C show important weight losses corresponding to the oxidation of cobalt and molybdenum leading to $CoCr_2O_4$ and $CoMoO_4$ formation.

1. INTRODUCTION

Wear resistant and corrosion-resistant materials for industrial application in the presence of a deposit of salt or ash [1] molten glasses [2-5] or for gas turbine applications [6-10] need the development of high temperature resistant cobalt-based alloys [11-12]. The cobalt-based Phynox substrate is an iron-containing alloy. Iron additions in the range 5 to 15 wt. % on the microstructure and properties of two Co-Mn-Cr-Si wear resistant alloys (Tribaloys T400 and T800) were investigated [13]. Iron additions were found to stabilize the fcc form of the cobalt solid solution, to give a fully eutectic matrix and to decrease the volume fraction of the primary laves phase. These microstructural modifications have little effect on the strain fracture toughness but result in a significant increase in the modulus of rupture. Iron addition induces only minor changes in the corrosion and oxidation resistance. The oxidation behaviour of a Co-based Tribaloy T-800 (Co-17.5Cr-28.5Mo-3.4Si, wt.%) isothermally exposed in air, at 800 and 1000°C were investigated by Zhang [14]. Results indicated that the oxidation mechanism was dependent on the exposure temperature. The present work focuses on the oxidation behaviour of a carbide free Co-based Phynox alloy, in air, between 800 and 1100°C.

2. EXPERIMENTAL

A cobalt-based superalloy (Phynox), provided by ArcellorMittal Imphy was used in the present study. Its chemical composition (in wt. %) is given in table 1. The rectangu-

lar specimens are 1.6 mm thick and show a total surface area of about 5 cm^2. They were polished on silicon carbide paper up to the 1200 polishing grade, then washed with alcohol and finally dried just before oxidation between 800 and 1100°C. The kinetic results under isothermal conditions were recorded with a Setaram TG-DTA 92-1600 microthermobalance, for 24 h, in flowing laboratory air (1.2 vol.% H_2O). Thermal cycling tests were performed in static laboratory air at atmospheric pressure in a tubular furnace at 900, 1000 or 1100°C. Three samples were placed at the same time into an alumina crucible to estimate the reproducibility. Thermal cycles consist in a twenty hours exposure at high temperature, followed by four hours at ambient temperature after air quenching. The weight change of the samples was determined after each cycle on a balance with 0.01 mg accuracy. The characterization of the oxide scales was carried out in an X-ray Philips X' PERT MPD diffractometer (copper radiation, $\lambda_{K\alpha}$ = 0.15406 nm). The X-ray diffraction (XRD) conditions were: 2Θ scan, step 0.02°, range from 10 to 80°, 3 s counting time. The surface scale morphology and the cross sections were observed respectively with secondary electrons or back scatter electrons using a JEOL 7600 Scanning Electron Microscope (SEM). The analysis of the scale was performed with a LINK energy dispersive X-ray spectroscopy (EDX). The EDX point analyses were performed with an electron probe focused to a 1 μm spot.

Table 1. Phynox composition in wt. %

Phynox	Co	Cr	Ni	Fe	Mo	Mn	Si	Al	C	Ti	Nb	S
Content wt.%	Balance	20.4	15.1	14.1	7.1	1.85	0.43	0.04	0.042	0.007	<0.005	<0.005

3. RESULTS

Thermogravimetric measurements were isothermally carried out for 24 hours, at 800, 900, 1000, 1100°C, in air. Mass gain curves per unit area are given on Fig. 1. During the Cobalt-based Phynox oxidation all, the kinetic curves show a parabolic shape.

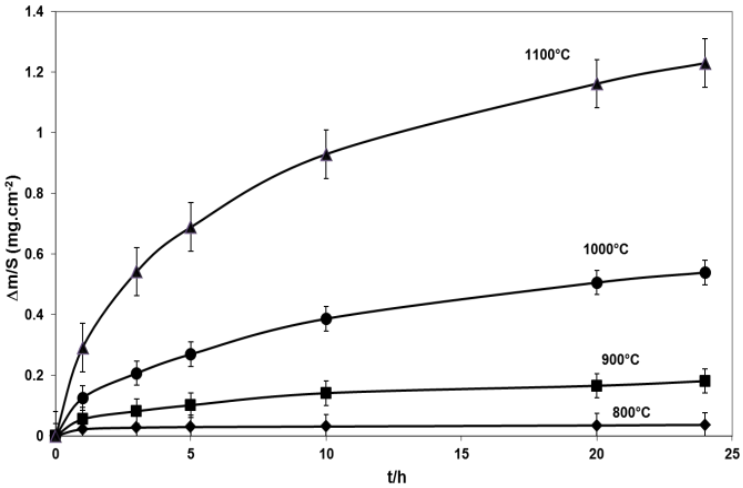

Fig. 1. Mass gain curves obtained during the isothermal cobalt base Phynox oxidation between 800 and 1100 °C, in air.

The calculated parabolic rate constants are reported in table 2. It indicates that the oxidation rate grows with increasing temperature.

Table 2. Calculated parabolic rate constants after isothermal Phynox oxidation, in air.

T (°C)	800	900	1000	1100
kp (g^2 cm^{-4} s^{-1})	1.68 (±0.05) 10^{-14}	3.78 (±0.05) 10^{-13}	3.20 (±0.05) 10^{-12}	1.66 (±0.05) 10^{-11}

Oxide scales formed on after 24 hours isothermal oxidation were analyzed by XRD on the metallic substrate after cooling to room temperature. The X-ray diffraction patterns show the presence of $Mn_{1.5}Cr_{1.5}O_4$ (ICDD 33-0892) and Cr_2O_3 (ICDD 38-1479). It appears that both oxides are present simultaneously on the specimen surface. The relatively high $Mn_{1.5}Cr_{1.5}O_4$ peaks intensity is not due to a higher proportion of this oxide in the scale but to the location of this oxide at the external interface. The underlying alloy diffraction peaks are less intense as temperature increases because the oxide scale is thicker. For each temperature the surface morphology of the scale formed on the Phynox specimens after 24 h isothermal oxidation, in air, shows that no scale spallation is observed on the surface obtained at 800 and 900°C (Fig.2). At 1000°C and 1100°C little parts of the external $Mn_{1.5}Cr_{1.5}O_4$ scale spalled off during cooling. The spallation of the external subscale occurred but the internal chromia scale remains adherent on the surface. In order to analyze the scale composition, EDX analyses of the sample surfaces were performed. It shows the presence of manganese, chromium, and oxygen in the outer subscale ($Mn_{1.5}Cr_{1.5}O_4$). EDX exhibits the presence of oxygen and chromium in the adherent subscale composed of Cr_2O_3.

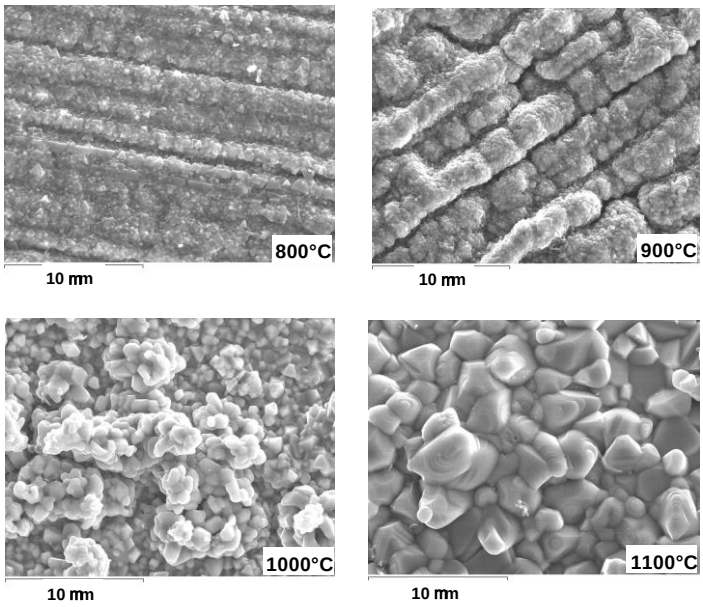

Fig. 2. Surface scale morphology after Phynox specimens oxididation at 800, 900, 1000, 1100°C, in air, after 24 hours.

SEM examinations were carried out on the specimen cross sections after isothermal oxidation, in order to estimate the subscale thickness and to identify the elements in the oxide scale (Fig. 3).

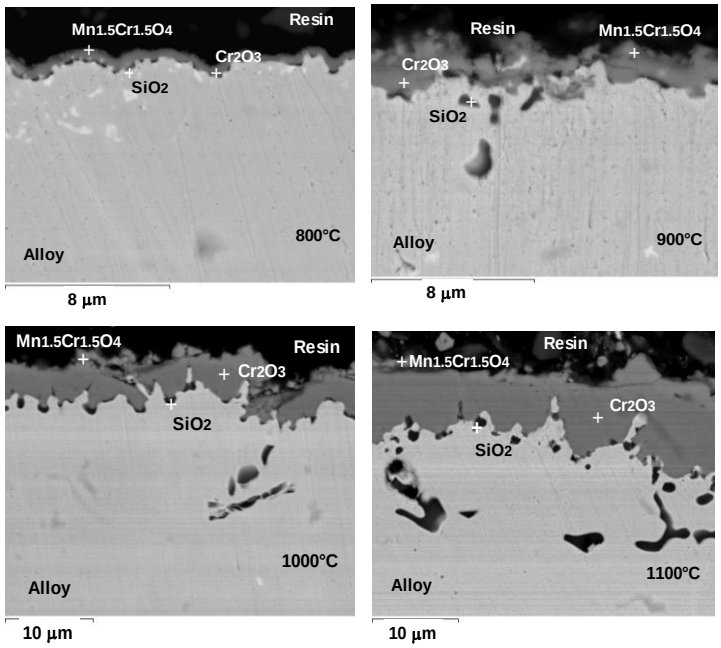

Fig. 3. SEM cross sections showing the morphology on the Phynox specimens oxidized at 800, 900, 1000, 1100°C, in air, after 24 hours (BSE).

After 24 h oxidation at 800°C, the adherent scale is about 1 µm thick. The manganese containing oxide is detected at the air/oxide interface. The main scale is composed of Cr_2O_3. The black spots at the internal interface correspond to SiO_2 precipitates. After oxidation at 900°C, the scale is about 4 µm thick. The manganese containing oxide is detected at the air/oxide interface. The main scale is composed of Cr_2O_3. SiO_2 is observed at the internal interface. After oxidation at 1000°C, EDX analyses show the presence of manganese at the external interface over a 8 µm thick Cr_2O_3 scale. Silicon oxide is located preferably in front of the internal chromia pegs. After oxidation at 1100°C, EDX analyses show the presence of manganese at the external interface. The main scale is composed of 11 µm thick Cr_2O_3. Silica is observed at the internal interface and along the alloy grain boundaries. No cobalt was detected inside the oxide scale after 24h oxidation between 800 and 1100°C. The oxide scale cross-section show that as temperature increases internal oxidation contributes to the scale formation.

On Fig. 4, mass changes registered during thermal cycling tests show that after 34 cycles the best behaviour is observed at 1000°C.

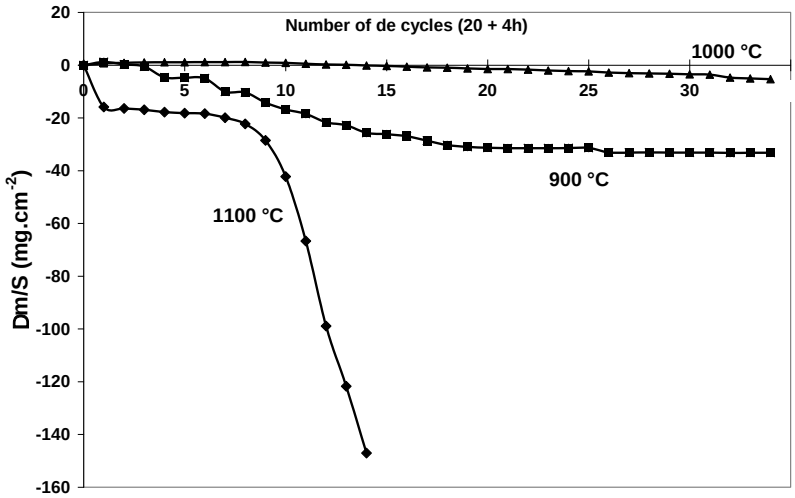

Fig. 4. Mass gain curves obtained during the thermal cycling test performed on a cobalt base Phynox oxidized between 900 and 1100 °C, in air.

At 900°C a weight loss corresponding to partial scale spallation is observed after only three cycles. At 1100°C, very important weight losses are registered from the beginning and especially after 8 cycles.

After 34 thermal cycles at 900°C, the scale still present on the surface is mainly composed of two spinel phases $CoCr_2O_4$ (ICDD 22-1084) and $Mn_{1.5}Cr_{1.5}O_4$ (ICDD 33-0892). Cr_2O_3 (ICDD 38-1479) oxide is also detected on the surface. After 34 thermal

cycles at 1000°C, chromia Cr_2O_3 (ICDD 38-1479) is well detected in the scale still present on the surface. The spinel phase is composed of $Mn_{1.5}Cr_{1.5}O_4$ (ICDD 33-0892). After 13 thermal cycles at 1100°C, the oxides formed differ from the one observed at lower temperatures. The scale is composed of $CoCr_2O_4$ (ICDD 22-1084) and $CoMoO_4$ (ICDD 25-1434). Cr_2O_3 (ICDD 38-1479) diffraction peaks are also detected on the surface.

After thermal cyclic oxidation, SEM-EDX analyses were performed on the specimen cross-sections to precise the oxide scale composition (Fig.5).

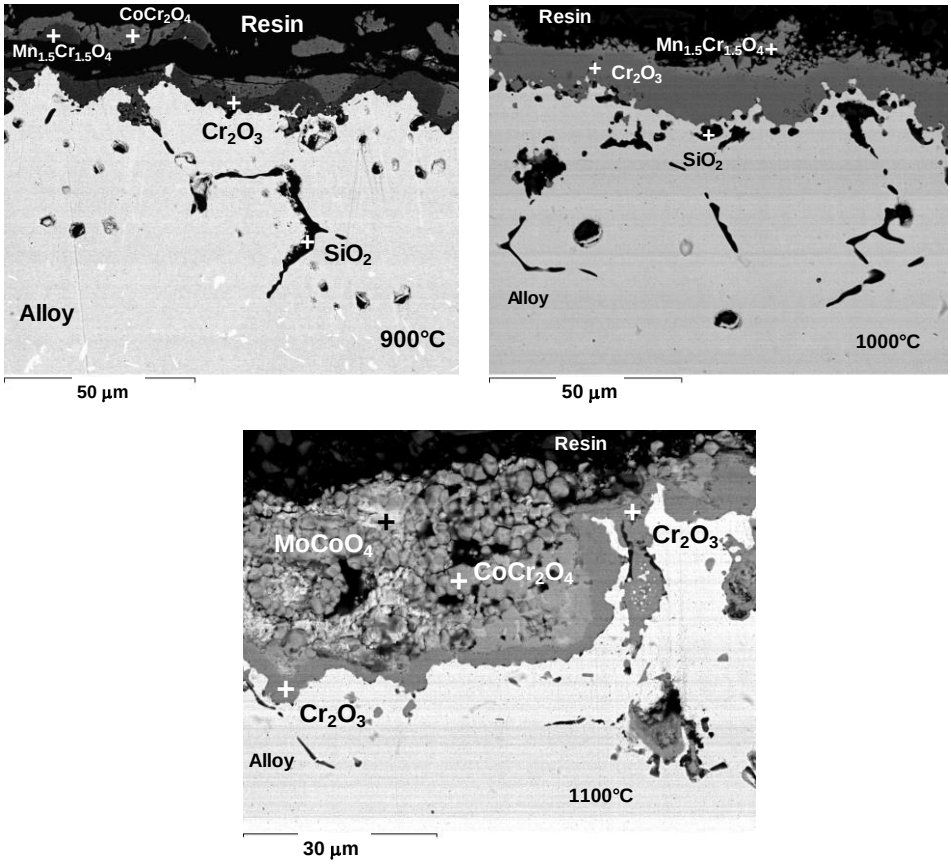

Fig. 5. SEM cross section showing the morphology on the Phynox specimens after 20 + 4 h thermal cycling in air. After 34 cycles at 900°C, after 34 cycles at 1000°C, after 13 cycles at 1100°C.

After 34 thermal cycles at 900°C, the cross section shows that some parts of the oxide scale are non-adherent. The spalled scale is composed of $CoCr_2O_4$, manganese chromite and chromia. The adherent part of the scale is mainly composed of Cr_2O_3. The black areas located 50 µm deep along the alloy grain boundaries correspond to the internal oxidation of silicon. After 34 thermal cycles at 1000°C, the cross section shows that the oxide scale is adherent. The scale is composed of an outer manganese chromite oxide

subscale and an inner Cr_2O_3 scale. Cobalt and molybdenum are not present in the corrosion products. Internal oxidation of silicon is observed 50 µm deep inside the alloy. After 13 thermal cycles at 1100°C, the oxide scale cross-section shows a more complicated structure. Cobalt and molybdenum are present in the corrosion products. The porous outer scale is composed of $MoCoO_4$ disseminated in the main $CoCr_2O_4$ scale. Cr_2O_3 is located as a thin oxide scale at the internal interface. Silica is found at the alloy grain boundaries as internal corrosion products.

4. DISCUSSION

Between 800 and1100°C kinetic results permit the calculation of the parabolic rate constants (kp) at each temperature.The Arrhenius plots of the kp values gives an apparent activation energy $E_a = 286 \pm 20$ kJ.mol^{-1}. It is close the values proposed in the literature [15-18] for the oxidation of chromia-forming alloys considering a diffusion-controlled mechanism by a continuous chromia scale. According to other authors E_a is ranging between 250 to 290 kJ.mol^{-1} in chromia scales. The E_a value and the X-ray diffraction results and SEM-EDX analyses are in accordance with a scale growth mechanism limited by a Cr_2O_3 scale acting as a compact and adherent diffusion barrier under isothermal conditions. The present results are different from those obtained by Zhang [14] because the alloying element content of the alloy T-800 is different from the Phynox one. Results showed that an external manganese chromite subscale was present after isothermal oxidation. Manganese chromite limits the chromia scale evaporation at temperatures higher than 1000°C [19]. Manganese outward diffusion to the scale external interface was also reported by authors [20-22]. The role of manganese in the oxidation process can be important. Some authors indicated that $Mn_{1.5}Cr_{1.5}O_4$ is not protective because it presents a porous and non-protective structure [20, 23]. Other authors pointed out that $Mn_{1.5}Cr_{1.5}O_4$ located at the external interface, could reduce the conversion of Cr_2O_3 into a CrO_3 volatile oxide above 1000°C [24-26]. Our study shows that manganese provides a beneficial effect during the isothermal exposure by hindering the chromia scale volatilisation at 1100°C. Nevertheless, under thermal cycling conditions the $Mn_{1.5}Cr_{1.5}O_4$ located at the external interface spalled off easily, the protection against volatilisation is lost and chromium depletion occurs leading to cobalt oxidation.

Previous studies discussed the role of molybdenum on the corrosion behavior of a Cr_2O_3-scale former at high temperatures. Molybdenum is generally added into steels as a solid-solution strengthener. But, with respect to the oxidation resistance, molybdenum can be undesirable because MoO_3 tends to melt at moderate temperature (795°C) [27]. On the other hand, silicon effect has been more extensively examined on chromia forming alloys. Even though too high an amount of silicon is considered as detrimental for the steels mechanical properties [28], its addition generally improves the oxidation resistance. Some authors stated that silicon segregates at the oxide/alloy interface and blocks the outward iron cationic diffusion [29-31]. Silicon is then present as a silica film, which lowers the steel oxidation rate. The high oxygen affinity of silicon also al-

lows its internal oxidation, developing SiO_2 precipitates at the internal interface [21, 32]. Then, it is reported that silica acts as a diffusion barrier and also leads to a chromia scale keying on the substrate due to an internal oxidation process [33, 34]. Silica also lowers the porosity at the internal interface acting as vacancies sinks [35]. Silicon also reduces the amount of non-protective iron oxides inside the scale [36] and hinders the iron rich nodule formation [30]. In the present work, the alloy silicon content is 0.43 wt.% and silica forms as internal oxide nodules and along the alloy grain boundaries. Internal silicon oxide seems to be preferably located in front of the internal chromia pegs then leading to a chromia scale keying on the substrate.

After thermal cycling tests at 1100°C, cross-sectional examination showed that molybdenum is present in the oxide scale as $CrMoO_4$ (Fig. 5). At lower temperatures molybdenum is not oxidized and no traces of the $CrMoO_4$ oxide are found in the scale. It is due to the fact that at low temperatures molybdenum remains non-oxidized and starts to oxidize at temperatures higher than 1100°C [17,18, 37]. It should also be noticed that in accordance with our results molybdenum promotes a keying effect of the chromia scale in the metallic substrate at temperatures lower than 1100°C [17,18, 37]. The best scale adherence observed at 1000°C is due to silicon oxide filling the vacancies generated at the internal interface by the outward chromium and manganese cation diffusion through the oxide scale. It is known that at low temperatures the volume fraction of SiO_2 is 180% larger than silicon [38-41]. It has also been proposed that a Mo-Si–O amorphous phases could form instead of SiO_2 and will show better protective properties [42]. At low temperature the effect of an amorphous phase can be envisaged at the oxide/steel interface where molybdenum has been detected. Molybdenum shows a quantitative effect on the oxidation protection without the over-doping effects encountered with the highest silicon containing steels [43].

Thermal cycling tests show that the less bad scale adherence is found at 1000°C (Fig. 4). This temperature appears to be the optimal temperature for a rapid chromium supply from the substrate and a thick protective chromia scale formation (Fig. 5). Authors indicated that on Co-Cr alloys the growth of CoO was faster than of Cr_2O_3 at low temperatures. This can explain the cobalt oxidation observed during thermal cycling at 900°C. At 900°C, the spinel oxide $Mn_{1.5}Cr_{1.5}O_4$ is not adherent and the non-protective $CoCr_2O_4$ is found in the oxidation products. When the temperature is raised, chromium diffusion becomes higher than cobalt diffusion [44]. Our results show that at 1000°C the chromia scale formation is favored and hinders the cobalt and molybdenum oxidation. Then, void accumulation at the internal interface is limited and a good chromia scale adherence is observed. At 1100°C thermal cycling conditions lead to the scale spallation and chromium depletion. Then, important weight losses are registered. The bad scale adherence observed is due to the molybdenum, chromium and cobalt oxidation to form $CoCr_2O_4$ and $CrMoO_4$ leading to void accumulation at the internal interface. Thermal cycling at 1100°C induces the $Mn_{1.5}Cr_{1.5}O_4$ spallation, the conversion of Cr_2O_3 into a CrO_3 volatile oxide can be expected leading to the protection loss [24-26].

5. CONCLUSIONS

High temperature oxidation of a cobalt based Phynox alloy show a parabolic rate law in the 800-1100°C temperature range under isothermal conditions. The scale growth mechanism of the cobalt based Phynox alloy in air at temperatures ranging between 800 and 1100°C is consistent with a growth mechanism limited by the diffusion process in a growing Cr_2O_3 oxide scale. Results show also that $Mn_{1.5}Cr_{1.5}O_4$ external subscale spall off easily after the highest temperature oxidation tests and cooling down to room temperature. Thermal cycling tests show that the less bad scale adherence is found at 1000°C. This good adherence can be related to a keying effect at the internal interface promoted by the presence of silicon and molybdenum. The good adherence is also due to a sufficiently high temperature permitting a rapid chromium supply from the substrate to maintain a thick continuous chromia scale. Thermal cycling at 900°C leads to te $CoCr_2O_4$ formation and a bad oxide scale adherence because cobalt oxidation is favoured at low temperature. At 1100°C thermal cycling conditions promotes the scale spallation and chromium depletion. Important weight losses are registered due to the cobalt and molybdenum oxidation.

REFERENCES

[1] Singh H., Gitanjaly S., Singh S., Prakash S., Applied Surface Science **255** (2009) 7062-7069.
[2] Berthod P., Lemoine P., Aranda L., Mater. Sci. Forum **595-598** (2008) 871-880.
[3] Berthod P., Michon S., Aranda L., Mathieu S., Gachon J.C., Computer Coupling of Phase Diagrams and Thermochemistry **27** (2003) 353-359.
[4] Di Martino J., Rapin C., Berthod P., Podor R., Steinmetz P. Corros. Sci. **46 (**2004)1865-188.
[5] Berthod P., Michon S., Di Martino J., Mathieu S., Noël S., Podor R., Rapin C., Computer Coupling of Phase Diagrams and Thermochemistry **27 (**2003) 279-288.
[6] Sahraoui T., Fenineche N. E., Montavon G., Coddet C. Journal of Materials Processing Technology **152** (2004) 43-55.
[7] Tobar M.J., Amado J.M., Alvarez C., Garcia A., Varela A., Yanez A., Surf. Coat. Technol. **202** (2008) 2297-2301.
[8] Navas C., Cadenas M., Cuetos J.M., De Damborenea J. Wear **260** (2006) 838 -846.
[9] Baxter D.J., Gilliland D., Lanza F., Toledo G.P., Bregani F., Mater. Sci. Forum **251-254** (1997) 801-808.
[10] Sahraoui T., Feraoun H.I., Fenineche N., Montavon G., Aourag H., Coddet C., Materials Letters **58** (2004) 2433-2436.
[11] Michel G., Berthod P., Vilasi M., Mathieu S., Steinmetz P., Surf. Coat. Technol. **205**, (2011) 3708-3715.
[12] Michel G., Berthod P., Vilasi M., Mathieu S., Steinmetz P., Surf. Coat. Technol. **205**, (2011) 5241-5247.
[13] Halstead A., Rawlings R.D., J. Mater. Sci. **20** (1985) 1693-1704.
[14] Zhang Y.-D., Yang Z.-G., Zhang C., Lan H. Oxid. Met. **70** (2008) 229-239.
[15] Chen J.H., Rogers P.M., Little J.A., Oxid. Met. **47 (**1997) 381-410.
[16] Hagel W.C., Seybolt A.U. J. Electrochem. Soc. **108 (**1961)1146-1152.

[17] Buscail H., El Messki S., Riffard F., Perrier S., Cueff R., Caudron E., Issartel C., Mat. Chem. Phys. **111 (**2008) 491-496.
[18] Buscail H., El Messki S., Riffard F., Perrier S., Cueff R., C. Issartel, J. Mater. Sci. **43** (2008) 6960-6966.
[19] Holcomb G.R., Alman D.E., Scripta Materialia **54 (**2006)1821-1825.
[20] Grübmeier H.B., Naoumidis A., Schulz H.A., J. Vac. Sci. Tech. **A4 (**1986) 2565-2574.
[21] Landkof M., Levy A.V., Boone D.H., Gray R., Yaniv E., Corros. Sci. **41** (1985) 344-357.
[22] Saeki I., Saito T., Furuichi R., Konno H., Nakamura T., Mabuchi K., Itoh M., Corros. Sci. **40** (1998) 1295-1302.
[23] Hussain N., Shahid K.A., Khan I.H., Rahman S., Oxid. Met. **43 (**1995) 363-378.
[24] Tedmon C.S., J. Electrochem. Soc. **113 (**1966) 766-768.
[25] Ben Abderrazik G. , Moulin G., Huntz A.M., Oxid. Met. **33 (**1990) 191-203.
[26] Tawancy H.M., Oxid. Met. **45 (**1996) 323-348.
[27] Wang Xu, Wang Lan-fang, Zhu Mei-li, Zhang Jun-shan, Lei Ming-kai, Trans. Nonferrous Met. Soc. China **16** (2006) 676-680.
[28] Armanet F., Davidson J.H., 'Les aciers inoxydables' (1990) Lacombe P., Baroux B., Beranger G. (Eds), Les Editions de Physique, Les Ulis France pp449-489.
[29] Basu S.N., Yurek G.J., Oxid. Met. **36 (**1991) 281-298.
[30] Huntz A.M., Material Science and Engineering, **A201 (**1995) 211-228.
[31] Evans H.E., Hilton D.A., Holm R.A., Webster S.J., Oxid. Met. **19** (1983) 1-18.
[32] Aguilar G., Larpin J.P., Colson J.C., Mémoires et Etudes Scientifiques-Revue de Métallurgie, (1992) 447.
[33] Durham R.N., Gleeson B., Young D.J., Oxid. Met., **50 (**1998) 139-165.
[34] Seal S., Bose S.K., Roy S.K., Oxid. Met. **41 (**1994) 139-178.
[35] Nagai H., Materials Science Forum, **43 (**1989) 75-130.
[36] Pérez F.J., Cristobal M.J., Hierro M.P., Pedraza F., Surface and Coatings Technology, **120-121 (**1999) 442-447.
[37] Buscail H., El Messki S., Riffard F., Perrier S., Issartel C., Oxid. Met. **75 (**2011) 27-39.
[38]. Meier G. H., Oxidation of Intermetallics **12 (**2004) 779-786.
[39] Chou T.C., Nieh T.G., Scripta Metallurgica et Materialia, **27** (1992) 1637-1646.
[40] Chou T.C., Nieh T.G., Scripta Metallurgica et Materialia, **26 (**1992) 19-27.
[41] Chou T.C., Nieh T.G., Journal of Materials Research, **8** (1993)1605-1620.
[42] Yanagihara K., Przybylski K., Mauryama T., Oxid. Met., **47** (1997) 277-285.
[43] Evans H.E., Hilton D.A., Holm R.A., Webster S.J., Oxid. Met. **19** (1983) 1-18.
[44] Kofstad P., 'High temperature corrosion' 1988, Elsevier Applied Science Publishers LTD, London and New York.